J. exp. Biol. ***196****, 77–92 (1994)*
Printed in Great Britain © The Company of Biologists Limited 1994

IONIC CIRCUIT ANALYSIS OF K^+/H^+ ANTIPORT AND AMINO ACID/K^+ SYMPORT ENERGIZED BY A PROTON-MOTIVE FORCE IN *MANDUCA SEXTA* LARVAL MIDGUT VESICLES

FRANCIS G. MARTIN

Department of Biology, Immaculata College, Immaculata, PA 19345, USA

AND WILLIAM R. HARVEY

Department of Biology, Temple University, Philadelphia, PA 19122, USA

Summary

Amino acid/K^+ symport (cotransport) across a model epithelium, the lepidopteran midgut, is energized by an electrogenic H^+ V-ATPase (H^+ pump) in parallel with an electrophoretic K^+/H^+ antiporter (exchanger). Attempts to analyze this process using well-known equilibrium thermodynamic equations (Nernst, Gibbs), diffusion equations (Nernst, Planck, Einstein, Goldman, Hodgkin, Katz) and equations based on Ohm's law (Hodgkin, Huxley) have all encountered major difficulties. Although they are useful for analyzing nerve/muscle action potentials, these state equations assume that brief perturbations in membrane conductance, g_m, and membrane voltage, V_m, occur so rapidly that no other parameters are significantly disturbed. However, transport studies often extend for minutes, even for hours. Perturbation of one parameter in complex transport systems invariably results in a state change as all of the other elements adjust to the prolonged stress.

The development of a comprehensive mathematical treatment for transport systems that contain pumps and porters (transporters) has been hampered by the empirical nature of the concept of membrane permeability and conductance. The empirical definition of permeability was developed before pumps and porters were known. Thus, 'permeability' is a gross parameter that, in practice if not in theory, could describe all transport pathways including pumps, porters and channels. To surmount these difficulties, we have applied ionic circuit analysis to vesicular systems containing insect midgut transport proteins. In this analysis, pumps, porters and channels, as well as ionic concentration gradients and membrane capacitance, are components of ionic circuits that function to transform metabolic energy (e.g. from ATP hydrolysis) into useful metabolic work (e.g. amino acid uptake). Computer-generated time courses reproduce key aspects of the coupling of the proton-motive force generated by an H^+ V-ATPase to $K^+/2H^+$ antiport and amino acid/K^+ symport in the lepidopteran midgut.

Introduction

We describe here a membrane biologist's 'theory of everything', which applies to the coupling between pumps, porters and channels in bacterial cells, intracellular organelles,

Key words: ionic circuit analysis, pumps, porters, compartmental capacitances, energy transduction, membrane transport, nutrient absorption, amino acid absorption, H^+ V-ATPase, H^+ pump.

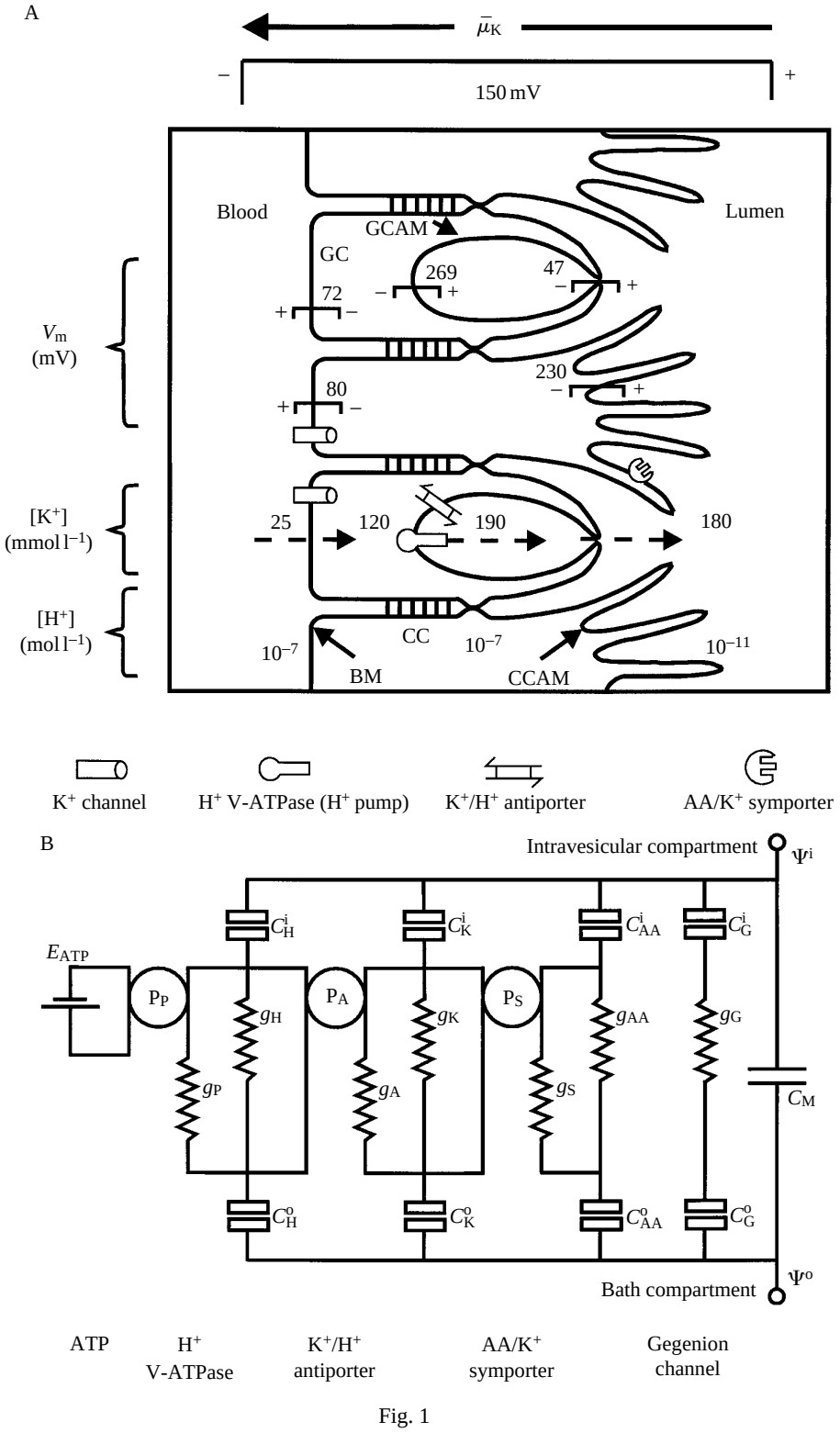
A
$\bar{\mu}_K$
150 mV
Blood
Lumen
GCAM
GC
269
47
72
230
80
V_m (mV)
[K+] (mmol l−1)
25
120
190
180
[H+] (mol l−1)
10−7
CC
10−7
10−11
BM
CCAM
K+ channel
H+ V-ATPase (H+ pump)
K+/H+ antiporter
AA/K+ symporter
B
Intravesicular compartment
Ψ^i
C_H^i
C_K^i
C_{AA}^i
C_G^i
E_{ATP}
P_P
P_A
P_S
g_H
g_K
g_{AA}
g_G
g_P
g_A
g_S
C_M
C_H^o
C_K^o
C_{AA}^o
C_G^o
Bath compartment
Ψ^o
ATP
H+ V-ATPase
K+/H+ antiporter
AA/K+ symporter
Gegenion channel

Fig. 1

plasma membrane vesicles and even in multicellular epithelia. Transporting cells, on the one hand, and signalling cells, on the other, are at opposite ends of the flux/voltage spectrum. Epithelial cell membranes, energized by highly regulated ATPases, pass large ionic fluxes with little change in membrane voltage, V_m, whereas signalling membranes, energized by ion gradients, pass tiny fluxes with large changes in V_m. Transporting membranes of bacterial cells, eukaryotic organelles and membrane vesicles are like those of epithelial cells in that they can sustain large fluxes at constant V_m. Yet membrane transport theories for epithelia, organelles and vesicles are usually patchwork modifications of the Hodgkin–Huxley theory for signalling membranes. Terms for pumps and porters are 'added on' to equations that were designed to deal with transient openings and closings of channels. We propose to start afresh. We will follow the strategy of Hodgkin and Huxley, but we will replace awkward concepts by tractable ones and emerge with a comprehensive, quantitative treatment for integrated membrane transport events.

The lepidopteran midgut (Fig. 1A) is a particularly useful model for this fresh start because it is very different from well-known mammalian systems and from the squid axon model (Harvey *et al.* 1986). V_m is not a combination of Na^+ and K^+ diffusion potentials, but is a component of an H^+ pump potential. In fact, no Na^+/K^+-ATPase is detectable in the basal or lateral membranes or any other membranes of the midgut epithelium; instead, an electrogenic H^+ V-ATPase (H^+ pump) energizes the apical membrane directly (Wieczorek *et al.* 1989). The $[Na^+]$ is low both inside the cells and in the lumen. The transapical V_m is approximately 240 mV, lumen positive. The ΔpH is 4, outside alkaline. The $[K^+]$ is high in the extracellular space on the apical side (lumen) and the K^+_{lumen}/K^+_{cell} activity ratio is maintained at approximately 1, despite massive K^+ transport from cell to lumen *in vivo*. Although electrical forces drive massive $K^+/2H^+$ antiport (Wieczorek *et al.* 1991; Lepier *et al* 1994) and amino acid/K^+ symport across the apical membrane, they do not significantly change the transapical V_m (see reviews in Harvey and Nelson, 1992).

In many of these respects, the lepidopteran midgut more closely resembles plant or bacterial membranes than classical animal cell membranes. The membrane is energized by a proton-motive force, not a sodium-motive force. Indeed a V_m generated by a proton-motive force is emerging as a common intermediate in many animal cells (Nelson, 1994). Already recognized as the primary energizer of endomembranes, H^+ V-ATPases are now recognized to be energizers of animal cell plasma membranes. The list already includes the apical membrane of all insect sensory epithelial cells and of many insect Malpighian tubule cells (Klein, 1992). It also includes frog skin mitochondria-rich cells (Ehrenfeld *et al.* 1989), two types of kidney cells (Brown *et al.* 1992), osteoclasts (Chatterjee *et al.*

Fig. 1. (A) Midgut model showing columnar cells (CC), columnar cell apical membranes (CCAM), basolateral membranes (BM), goblet cells (GC) and goblet cell apical membrane (GCAM), Also shown are typical voltages (in mV), ion gradients (in $mmol\,l^{-1}$) and transporters. $\bar{\mu}_K$, electrochemical potential difference for potassium (after Harvey *et al.* 1986). (B) Circuit diagram of a hypothetical vesicular system. Abbreviations are explained in the text.

1992) and macrophages (Grinstein *et al*. 1992). Membranes energized by a proton-motive force using V_m as a common intermediate may eventually turn out to be more important, even in animal cells, than membranes energized by a sodium-motive force using ion gradients as an intermediate.

Hodgkin–Huxley strategy in retrospect

The Hodgkin and Huxley (1952) equations were the 'jewels' in the mathematical 'crown' that allowed the reconstruction of squid axon action potentials from voltage-clamp data. This crown developed through the three stages described below.

Thermodynamic analysis

Thermodynamic analysis, based on Willard Gibbs chemical potential $\mu_i=\delta G/\delta n_{i|T,P,nj}$, provided a means for calculating the limits of diffusion phenomena (Snell *et al.* 1965). $\delta G/\delta n$ is the partial change in molar free energy attributable to the addition of 1 mole of one molecular species (i) to a compartment when temperature (T), pressure (P) and the number (n) of molecules of all other species (j) are not allowed to change. This potential allows us to think about what happens to a single solute species and to combine that result with what happens to other species that are the components of a chemical reaction, such as ATP hydrolysis.

For a non-electrolyte i:

$$\mu_i = \mu_i^o + \boldsymbol{R}T\ln c_i \tag{1}$$

and for an electrolyte k:

$$\bar{\mu}_k = \mu_k^o + \boldsymbol{R}T\ln c_k + z_k F\Psi\,, \tag{2}$$

where all terms are expressed in J mol^{-1}; μ_i is the chemical potential of a nonelectrolyte i, $\bar{\mu}_k$ is the electrochemical potential of an ionic species k; μ_i^o and μ_k^o are the standard chemical potentials of the nonelectrolyte and electrolyte, respectively; $\boldsymbol{R}$ is the universal gas constant (Boltzman's constant times Avogadro's number) and represents the vibrational, rotational and translational energy per mole of substance; T is the absolute temperature; c_i and c_k are the concentrations of i and k respectively; z is the valence of k with sign; F is Faraday's number and Ψ is the electrical potential expressed in volts. When an electrolyte is at equilibrium across a membrane, the μ_k^o terms cancel and, solving for the potential difference across the membrane, $\Delta\Psi$, we obtain the Nernst equation:

$$\Delta\Psi = E_k = (\boldsymbol{R}T/z_kF)\ln(c_k^o/c_k^i)\,, \tag{3}$$

or

$$\Delta\Psi = E_k = (\boldsymbol{R}T/z_kF)2.3\log(c_k^o/c_k^i)\,, \tag{3′}$$

where the superscripts o and i, in these equations, represent the outside and inside compartments of a cellular or vesicular system and E_k is the equilibrium voltage for k. At 25 °C for a monovalent cation, $\boldsymbol{R}T/z_kF$=25.7 mV, so a tenfold concentration ratio across a membrane is equivalent to a $\Delta\Psi$ of approximately 60 mV. In this equilibrium condition, $\Delta\Psi=E_k$ but in general $\Delta\Psi\neq E_k$.

Diffusion theory

Working with the Nernst–Planck–Einstein diffusion concepts, Goldman (1943) developed his 'constant field theory', which Hodgkin and Katz (1949) later used to derive an equation that describes the effects of ionic permeability (p) changes on membrane voltage (*E*):

$$E = \boldsymbol{R}T/F\ln \frac{p_{\mathrm{K}}[\mathrm{K}^+]^{\mathrm{o}} + p_{\mathrm{Na}}[\mathrm{Na}^+]^{\mathrm{o}} + p_{\mathrm{Cl}}[\mathrm{Cl}^-]^{\mathrm{i}}}{p_{\mathrm{K}}[\mathrm{K}^+]^{\mathrm{i}} + p_{\mathrm{Na}}[\mathrm{Na}^+]^{\mathrm{i}} + p_{\mathrm{Cl}}[\mathrm{Cl}^-]^{\mathrm{o}}}. \tag{4}$$

This equation, commonly known as the Goldman equation, was used by Hodgkin and Katz for a quantitative explanation of squid axon resting potentials.

Equivalent circuit analysis

In their analysis of action potentials, however, Hodgkin and Huxley concluded that the difficulties in determining millisecond changes in permeability coefficients would be insurmountable. They circumvented the problem by using an equivalent circuit and Ohm's law to derive an equation which they applied to nerve signalling (Hodgkin and Huxley, 1952):

$$I = C_{\mathrm{m}}\mathrm{d}V/\mathrm{d}t + \bar{g}_{\mathrm{K}}n^4(V - V_{\mathrm{K}}) + \bar{g}_{\mathrm{Na}}m^3h(V - V_{\mathrm{Na}}) + \bar{g}_{\mathrm{l}}n^4(V - V_{\mathrm{l}})\,, \tag{5}$$

where they used I to represent the total membrane current, C_{m} the membrane capacitance, V the membrane voltage, t the time, $\bar{g}_{\mathrm{K}}$, $\bar{g}_{\mathrm{Na}}$ and $\bar{g}_{\mathrm{l}}$ the maximal K^+, Na^+ and leakage conductances, respectively, n, m and h, variable empirical coefficients, and V_{K}, V_{Na} and V_{l} the equilibrium potentials for each of the ions.

This approach of Hodgkin and Huxley was so successful that it led to a Nobel Prize and dominated subsequent thought concerning transport physiology. However, its very success may have been unfortunate for scientists attempting to deal with complex systems including pumps and porters as well as channels. Attempts to modify the Hodgkin–Huxley equations (developed for nerve and muscle membranes containing fast-opening and fast-closing channels) in order to obtain a mathematical treatment suitable for transporting epithelia (containing pumps, porters and chronically open channels) have met with limited success. The state equations of Nernst, Goldman and others do not consider the presence of pumps and porters. Mullens and Noda (1963) added a factor to the Goldman equation to include the effects of an electrogenic ion pump on the membrane potential. Others have modified variations of the Hodgkin–Huxley equation to solve for V_{m} in the presence of electrogenic pumps (see Kishimoto *et al.* 1981). However, the effects of porters on electrical parameters have never been adequately addressed. Gerencser and Stevens (1994) address this problem in this volume, using non-equilibrium thermodynamics (Kedem and Katchalsky, 1958) to analyze transport in animal cells. We address the problem here, using circuit analysis techniques (Blitzer, 1964; Edminister, 1965) to examine transport in lepidopteran midgut components.

As can be seen from the previous paragraphs, the symbols representing membrane voltage are different for each set of workers. Along with Hodgkin and Katz's E and Hodgkin and Huxley's V, the symbols E_{m} and V_{m} are often used to represent the

membrane voltage. E_k and V_k have both been used to represent ionic equilibrium potentials. In the equations that follow, $\Delta\Psi$ represents theoretically calculated membrane voltages and V_m empirically measured membrane voltages. The symbol E with a subscript represents equilibrium potentials for specific ions.

Classical thermodynamics of lepidopteran midgut ion homeostasis

The lepidopteran midgut has proved to be a favorable model for epithelial ion and metabolite transport. Its large size, enormous fluxes (Harvey and Nedergaard, 1964) and relatively simple structure (Anderson and Harvey, 1966) enabled a physiological and biochemical characterization of transport activities (reviews in Harvey and Nelson, 1992) that led to the identification (Wieczorek *et al.* 1989), as well as the cloning and sequencing of most of the major subunits of its plasma membrane H^+-translocating V-ATPase (Dow *et al.* 1992; Gill and Ross, 1990; Gräf *et al.* 1992, 1994*a*,*b*; Lepier *et al.* 1994; Novak *et al.* 1992; reviewed by Wieczorek, 1992).

Equilibrium thermodynamics has defined limits for pump-driven ion accumulation ratios in the lepidopteran midgut, just as it has defined limits for resting and action potentials in the squid axon. The relationship between the electromotive force available from ATP hydrolysis and the ionic distributions coupled to the hydrolysis by an ATPase is obtained by equating the energy available from ATP hydrolysis to the energy used to create ion gradients:

$$\Delta G_{ATP}/nz_kF = \bar{\mu}_k/z_kF = \Delta\Psi + \boldsymbol{R}T/z_kF\ln(c_k^o/c_k^i)\,. \quad (6)$$

As it is in most cells, ΔG_{ATP} is held constant in the lepidopteran midgut by metabolic controls; its value was calculated from the split-beam spectrometer data of Mandel *et al.* (1980). Taking n, i.e. the ratio of molecules of ATP hydrolyzed to protons pumped, to be 1:2, the value for $\Delta G_{ATP}/nz_kF$ was calculated to be approximately 240 mV (Harvey, 1992). This 240 mV is the voltage rating for the midgut circuits driving secondary processes in the same sense that 220 V is the voltage rating for American household electrical circuits driving stoves and dryers. Writing equation 6 for each of the three principal ions (z_k=1 for all) in larval lepidopteran midgut at 25 °C produces the following:

$$\Delta G_{ATP}/2F = 240\,\text{mV} + 60\,\text{mV}\log\{[K^+]^o/[K^+]^i\}\,, \quad (6a)$$

$$\Delta G_{ATP}/2F = 240\,\text{mV} + 60\,\text{mV}\log\{[Na^+]^o/[Na^+]^i\}\,, \quad (6b)$$

$$\Delta G_{ATP}/2F = 240\,\text{mV} + 60\,\text{mV}\log\{[H^+]^o/[H^+]^i\}\,; \quad (6c)$$

the superscripts o and i represent the conditions in the lumen and the epithelial cell interior respectively. Empirical values for V_m of 200–270 mV have been measured across the lepidopteran midgut apical membrane (Dow and Peacock, 1989), implying that the tissue is operating near its thermodynamic maximum. The 240 mV, which corresponds to a 10 000-fold concentration ratio for each of the univalent cations under consideration, is theoretically feasible as demonstrated by Gerencser and Stevens (1994). The principal luminal cation in the lepidopteran midgut is K^+; $[K^+]$ in the lumen

is approximately 300 mmol l^{-1} and in the cells is approximately 120 mmol l^{-1}, but the activity coefficient is approximately 0.3 in the lumen and 0.7 in the cells, so $E_K \approx 0$ (Dow *et al.* 1984). Thus, K^+ is far from equilibrium and the 240 mV V_m drives K^+ into the cells. However, H^+ is virtually at equilibrium ($E_H \approx V_m$) across the apical membrane of midgut epithelial cells; the lumen pH is approximately 11 and the cell pH is 7; thus, ΔpH is approximately 4; and the calculated E_H of approximately 240 mV balances the measured V_m.

Ionic circuit analysis of pumps, porters and channels

At this point we must part company with Hodgkin and Huxley. A simple equivalent circuit, such as the one they used to derive equation 5, will not suffice to deal with changing pump, porter and channel conductances or with the resulting changes in transmembrane ionic currents, ionic equilibrium potentials and membrane voltages. Martin (1992) used circuit analysis based upon Kirchoff's laws as well as mesh and nodal analysis (Blitzer, 1964; Edminister, 1965) to develop a new theory of transport. He then wrote an algorithm that included not just channels, but pumps and porters as well, and used the algorithm to write a computer program. This analysis departs from all previous ones by representing ionic gradients as charged compartmental capacitances instead of batteries; the use of batteries is limited to the chemical driving force behind pumps.

Membrane capacitance and compartmental capacitance

Membrane capacitance, C_m, is the rate of accumulation of charge, Q, as V_m develops, $C_m = \delta Q/\delta V_m$. Because the dielectric thickness of all biological membranes is approximately 3 nm, the membrane capacitance has a constant value of about 1 μF cm^{-2}. By analogy, the compartmental capacitance, C_v, is the rate of accumulation of charge in a bulk compartment, such as the interior of a cell or a vesicle, as the concentration of an ion changes; $C_v = \delta Q/\delta E_k$. The δE_k term can be calculated from the Nernst equation (equation 3); in this case, $E_k = (\boldsymbol{R}T/z_kF)\ln(c_k^s/c_k^i)$, where c_k^i is the concentration of the ionic species in the compartment and c_k^s is the concentration under standard conditions, taken as 1 mmol l^{-1}, for convenience. The compartmental capacitance is clearly not a constant, but is a function of concentration, and therefore of volume; its value can range from less than 1 μF for a small vesicle to more than 1 MF for an intestinal lumen.

Just as the membrane capacitances depend upon the dielectric constant of the lipid bilayer, the compartmental capacitances depend upon a dielectric-like parameter, the activity coefficient of the ion under consideration. Unlike membrane capacitances, which are usually assumed to be linear and to remain constant under large changes in charge, compartmental capacitances are very nonlinear since they are very sensitive to the amount of charge present. As with all capacitances, compartmental capacitances combine with themselves and other capacitances to form series-parallel circuits.

Sequential versus *systematic analyses*

Transduction of energy in a membrane system is an integrated process, in which all ionic species contribute to the load on cell metabolism as transport work is being done. A

perturbation of one component in a system has the ability to affect the whole system. If a system consists of just two or three components, an intuitive or semiquantitative analysis can be undertaken. In such an approach, the action of one component sets up a condition, e.g. a concentration gradient or a transmembrane voltage, which then determines the action of a second component. If sufficient isolation exists between components, then such a sequential analysis may be adequate to treat the effects of one component or another component or two. However, if there are many components and/or if component activities are coupled, then such an intuitive and semiquantitative sequential approach rapidly becomes unwieldy if not impossible.

Ionic circuit analysis overcomes these difficulties. It provides a way to analyze quantitatively the complex interactions among the various components of complex membrane energy transduction systems *in vivo* or *in vitro*. Ionic circuit analysis is an extension of electrical circuit analysis which includes components that are unique to ionic circuits of biomembranes (Martin, 1992). Whereas equivalent electrical circuit analysis depicts systems metaphorically, ionic circuit analysis represents systems as they actually exist.

Circuit diagram of a hypothetical vesicular system

A circuit diagram of a hypothetical vesicular system, containing the major transporters found in the apical membranes of midgut cells, demonstrates the use of ionic circuit analysis (Fig. 1B). The main components are a proton-translocating V-ATPase (pump) (P_P), a K^+/H^+ antiporter (P_A) and an amino acid/K^+ symporter (P_S); each component containing a finite internal conductance (g_P, g_A and g_S) that limits its efficiency. Also present are specific transmembrane leakage conductances (e.g. uniporters, channels and slips) for each of the two major transported ions (g_H and g_K) and for the symported amino acids (g_{AA}). A fourth leakage conductance (g_G) deals with gegenions that are not specifically pumped or ported, but move through channels. Just as the membrane capacitance (C_m) is the linear capacitance formed by the two conducting aqueous solutions (intravesicular and bath) and the dielectric property of the lipid bilayer membrane that separates them, the ionic compartmental capacitances (C_H, C_K, C_G and C_{AA}) are the nonlinear capacitances of the intravesicular (i) and bath (o) compartments themselves, as defined above. The only power source for the system is the driving force of ATP hydrolysis, expressed as an electrical potential (E_{ATP}).

In ionic circuit analysis, leakage conductances and the membrane capacitance are standard components that are used in the same way as in equivalent electrical circuits. The pump, porters and compartmental capacitances, in contrast, are unique to ionic circuits. The pumps and porters are energy-transduction devices analogous to transformers in a.c. electrical circuits. They have primary and secondary sides depending on the direction of energy flow and are step-up or step-down transformers according to their stoichiometric coupling ratios. They are current-inverting if they are antiporters or current-noninverting if they are symporters. They can match impedances from one side to the other. The other components, the ion-specific compartmental capacitances, are the electrical manifestations of the solution compartments (see above). Just as the membrane capacitance is a function of the area and thickness of the membrane, the compartmental

capacitance is a function of the volume of the compartment. The compartmental capacitances shown in Fig. 1B are distinguished from the membrane capacitance by a different symbol. Unlike the two halves of the symbol for the membrane capacitance, the two halves of the symbol for compartmental capacitance are not meant to represent the aqueous compartments on either side of the membrane. A compartmental capacitance is the specific ionic capacitance of the compartment itself as explained above; hence, compartmental capacitances are shown for each ion on each side of the membrane. A comprehensive mathematical analysis of pumps and porters that uses such compartmental capacitances has been published previously (Martin, 1992).

Algorithm for the analysis of the hypothetical vesicular system

Using the circuit diagram in Fig. 1B as a foundation, an iterative program was written. The program depicts the flow of ionic currents, the formation of ionic activity gradients and the development of transmembrane voltage as they change over time. The program uses nodal network analysis, which takes advantage of two facts: (1) that all of the ionic pathways through the membrane are essentially in parallel with each other and (2) that the membrane voltage is a common force that affects the flow of all the ionic species involved. During each iterative step, the net current flow for each ionic species is calculated and the charges on the membrane and compartmental capacitances are then adjusted accordingly.

Each iterative step of the analysis begins with the calculation of E_k across the vesicular membrane. This is done for each species and each compartment using the number of ions present, the activity coefficients of the ions, and the volumes of the vesicle and the bath compartments. Each step also begins with the calculation of the $\Delta\Psi$ based upon the charge on the membrane capacitance (1 μF cm^{-2}).

The net current flow for a given ionic species is the sum of the current flows through all of the pump, porter and leakage pathways available to the ion. Current flow through the leakage pathway (I_{kl}) is calculated using the equation $I_{kl}=g_{kl}(\Delta\Psi-E_k)$, where $\Delta\Psi$ and E_k are the membrane voltage and the specific ionic equilibrium potential, respectively, and g_{kl} is the conductance of the pathway. The current through the pump pathway is calculated using the equation $I_{kP}=g_{kP}(\Delta\Psi-E_k-E_{ATP}/n)$, where I_{kP} is the current flow through the pump and n is the stoichiometric coupling ratio, i.e. the number of ions pumped per molecule of ATP hydrolysed.

Calculating the current flow through porters is a bit more complicated. It involves two different ionic species, k and j, one of which (assume it to be k) moves through the primary ($'$) side of the porter (left side in Fig. 1B) while the other (assume it to be j) moves through the secondary ($''$) side of the porter (right side in Fig. 1B). Also, one must consider the primary:secondary coupling ratio of the porter m; symporters have positive values of m whereas antiporters have negative values of m.

In order to determine the currents through a porter, one must consider energy transformation in both the forward (f) direction (left to right in Fig. 1B) and the reverse (r) direction (right to left in Fig. 1B). In the forward direction, a partial primary current flow, $I_{k'f}$, is calculated:

$$I_{k'f} = (g_{porter}/m^2)(\Delta\Psi - E_k)\,, \tag{7a}$$

where g_{porter} is the porter conductance assigned to the secondary side. Next, a partial secondary current flow, $I_{j''f}$, is calculated:

$$I_{j''f} = I_{k'f}/m\,. \tag{7b}$$

Once the forward energy transformation has been calculated, the reverse transformation is determined. A second partial secondary current flow, $I_{j''r}$ is determined:

$$I_{j''r} = g_{porter}(\Delta\Psi - E_j) \tag{7c}$$

and its coupled current, $I_{k'r}$, in the primary side of the porter is calculated,

$$I_{k'r} = I_{k''j}m\,. \tag{7d}$$

A given ionic species, e.g. *k*, could be in the primary side of one group of porters and in the secondary side of another group of porters (e.g. K^+ is in the secondary side of the H^+/nK^+ antiporter and in the primary side of the amino acid/K^+ symporter); hence, it could have both primary and secondary partial currents ($I_{k'f}$, $I_{k'r}$, $I_{k''f}$ and $I_{k''r}$). The net current flow for any ion, I_{kNet}, is the sum of the leakage currents, pump currents and partial currents through all their individual pathways:

$$I_{kNet} = I_{kl} + I_{kP} + I_{k'f} + I_{k''f} + I_{k'r} + I_{k''r}\,. \tag{8}$$

Multiplying the net ionic current by the duration of the iterative step increment and dividing the product by Faraday's constant yields the total flux for that species. Once the fluxes are known, the numbers of ions of each species in both compartments can be incremented or decremented depending on the directions of the fluxes. Adding all of the net ionic currents will yield the net membrane current. Multiplying this current by the duration of the iterative step increment determines the net change in the charge on the membrane capacitance. These new values then become the starting values for the next iteration.

Circuit analysis of different experimental conditions

In order to demonstrate the usefulness of the preceding algorithm, a program written in Pascal was used to plot the time courses of events in several different simulated experiments. The program allows the investigator to control all of the variables which could potentially change the results of an experiment. In all the simulated experiments depicted here, vesicles (1 μm in diameter) are bathed by a volume (1 ml per vesicle) of medium at room temperature (25 °C) and standard pressure (1 atmosphere=101.3 kPa). Fig. 1B is the general schematic diagram for all the experiments, but pathways not explicitly turned on in the description of the experiment are rendered inoperative by the assignment of a very low conductance (10^{-30} S cm^{-2}). Where the data were available, the values for component conductance and ionic activities were adjusted so that the computer-generated experiments were similar to actual laboratory experiments.

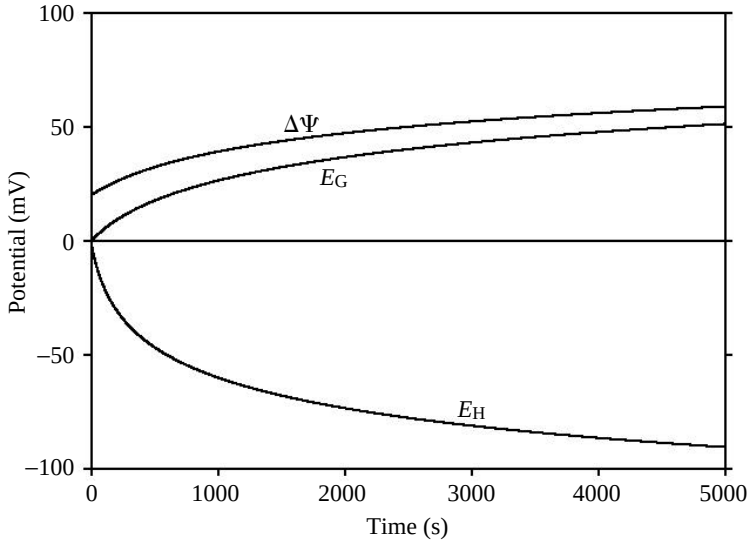

Fig. 2. H^+ V-ATPase with gegenion. $\Delta\Psi$, electrical potential difference; E_G, membrane potential for the gegenion; E_H, membrane potential for H^+.

H^+ V-ATPase with gegenion (acidification)

Fig. 2 shows the development of $\Delta\Psi$ and the equilibrium potentials for protons (E_H) and gegenions (E_G) across a vesicular membrane containing an H^+ V-ATPase (H^+ pump) ($g_P=10^{-7}\,S\,cm^{-2}$, n=2 protons per ATP) and a negative gegenion (G^-) pathway ($g_G=10^{-6}\,S\,cm^{-2}$). The initial solutions both inside and outside the vesicle are the same (the activity of $H^+=10^{-7}\,mol\,l^{-1}$ with an activity coefficient of 10^{-7} and activity of $G^-=50\,mmol\,l^{-1}$ with an activity coefficient of 10^{-2}. (Note that the dissociation of water is the primary source of protons in the examples described in this section and is the reason that the very low activity coefficient is assigned to H^+.) The plot shows the development of three different voltages, a negative E_H and positive E_G, and the membrane voltage $\Delta\Psi$. The negative E_H is to be expected from the acidification of the vesicular contents by the inwardly directed H^+ V-ATPase. Close examination reveals that $\Delta\Psi$ develops faster initially, but that its development slows and E_G approaches $\Delta\Psi$ as the experiment proceeds. This pattern arises because C_G is effectively in parallel with C_m but C_G charges through a lower conductance (series combination of g_P and g_G) than C_m (g_P alone). Since the parallel combination of C_G and C_m is in series with C_H, at equilibrium $\Delta\Psi=E_G$ and $\Delta\Psi+E_H=V_{ATP}/n$.

H^+ V-ATPase and K^+/H^+ antiporter in parallel (alkalization)

Fig. 3 shows the development of $\Delta\Psi$, E_H and E_K across a vesicular membrane containing an H^+ V-ATPase ($g_P=10^{-7}\,S\,cm^{-2}$, n=2 protons per ATP) and a K^+/H^+ antiporter ($g_A=10^{-7}\,S\,cm^{-2}$, $m=-2$ protons per K^+). The initial solutions both inside and outside the vesicle are the same [activity of $H^+=10^{-7}\,mol\,l^{-1}$ with an activity coefficient

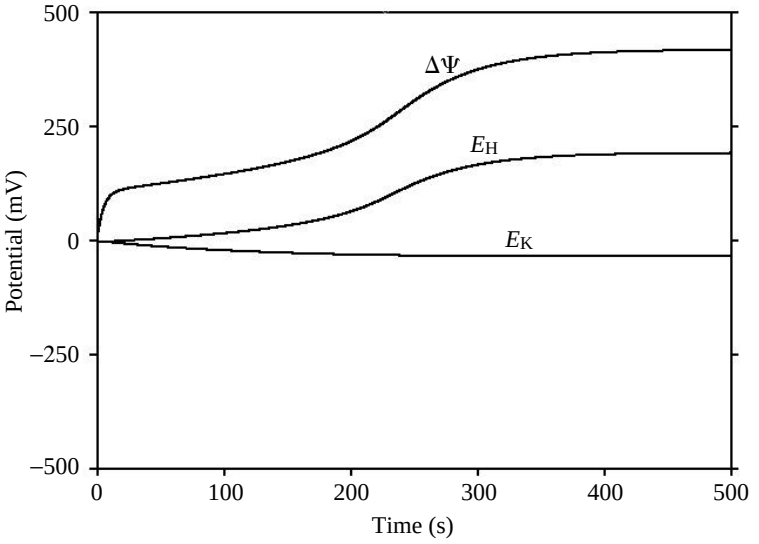

Fig. 3. H^+ V-ATPase and K^+/H^+ antiporter in parallel. Abbreviations as in Fig. 2.

of 10^{-7} (see note above) and activity of K^+=5 mmol l^{-1} with an activity coefficient of 10^{-2}]. The negative E_K is the result of potassium accumulation inside the vesicle as inwardly pumped protons move out through the antiporter. With no gegenion leakage in this experiment, all of the pump potential is developed across C_m ($\Delta\Psi=E_{ATP}/n$). The large $\Delta\Psi$ which results drives protons through the antiporter and out of the vesicle, leaving the vesicle contents alkaline.

Potassium-driven amino acid cotransport (AA/K^+ symport)

Fig. 4 shows the change in intravesicular K^+ and anionic amino acid (AA^-) activities in a system with an AA/K^+ symporter ($g_S=10^{-9}$ S cm^{-2}, m_S=1AA^- per K^+) in the vesicular membrane. Initial AA^- activity is the same in both the intravesicular and bathing solutions (5×10^{-4} mol l^{-1} with an activity coefficient of 1) but an initial K^+ gradient exists between the bathing medium (5×10^{-2} mol l^{-1} with an activity coefficient of 1) and the intravesicular compartment (5×10^{-4} mol l^{-1} with an activity coefficient of 1). As K^+ moves down its electrochemical gradient, it drives AA^- into the vesicle through the AA/K^+ symporter. However, as the K^+ electrochemical gradient dissipates, the accumulation of AA^- reaches a peak and then slowly reverses, coming to equilibrium at an activity higher than the initial, but lower than the peak, value. Amino acid uptake experiments performed by Hennigan *et al.* (1993*a*,*b*) show a similar pattern of K^+-driven amino acid accumulation over time.

H^+ V-ATPase, K^+/H^+ antiporter, AA/K^+ symporter and gegenion (amino acid uptake)

Fig. 5 shows the development of $\Delta\Psi$, E_H, E_K, E_G and E_{AA} across a vesicular membrane containing an H^+ V-ATPase ($g_P=10^{-7}$ S cm^{-2}, n=2H^+ per ATP), a K^+/H^+

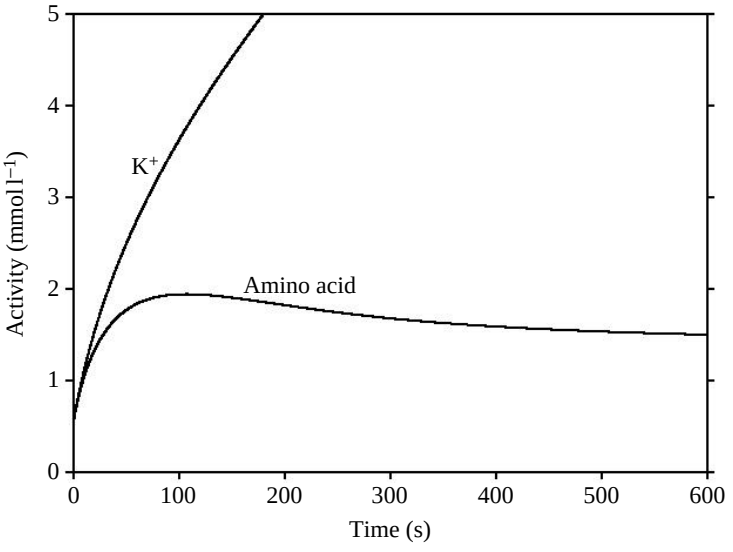

Fig. 4. Potassium-driven amino acid (AA) cotransport.

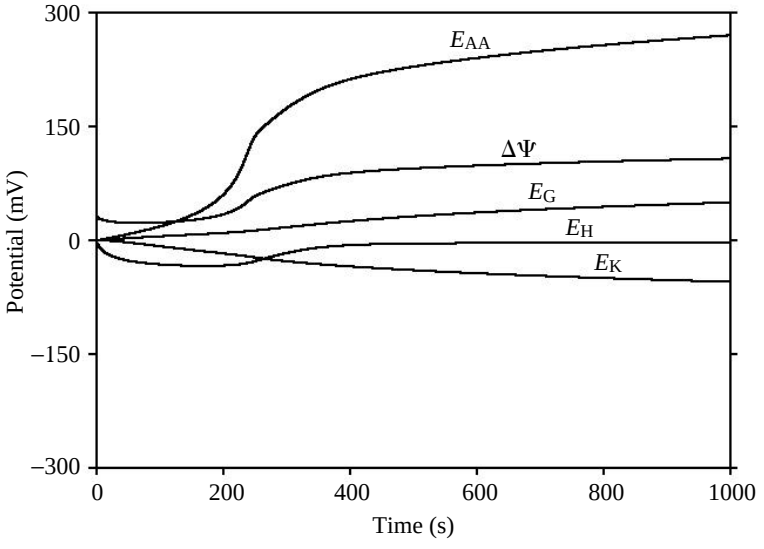

Fig. 5. H^+ V-ATPase, K^+/H^+ antiporter, AA/K^+ symporter and gegenion. E_{AA}, E_G, E_H and E_K, membrane potentials for amino acid, gegenion, H^+ and K^+, respectively; $\Delta\Psi$, electrical potential difference.

antiporter ($g_A=10^{-7}$ S cm^{-2}, $m_A=-2K^+$ per H^+), an AA/K^+ symporter ($g_S=10^{-7}$ S cm^{-2}, n=1AA per K^+) and a gegenion (G^-) leakage ($g_G=10^{-6}$ S cm^{-2}). The initial solutions both inside and outside the vesicle are the same [activity of $H^+=10^{-7}$ mol l^{-1} with an

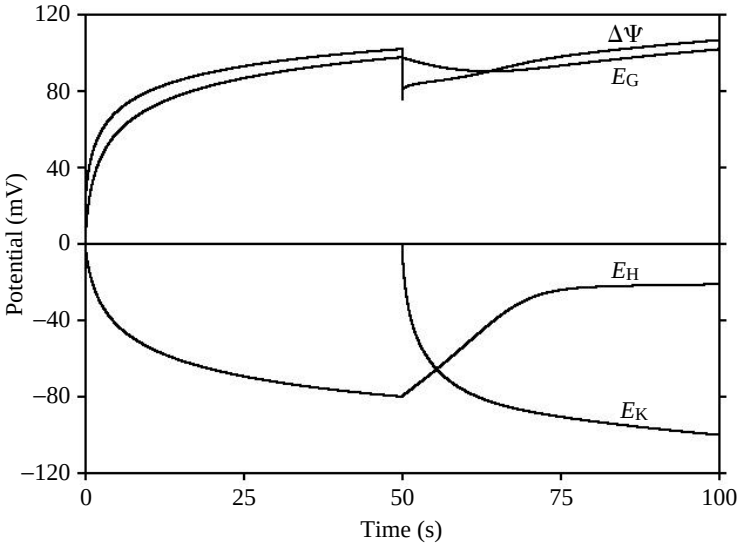

Fig. 6. H^+ V-ATPase, K^+/H^+ antiporter and gegenion with a switch. Abbreviations as Fig. 5.

activity coefficient of 10^{-7} (see note above) and the activities of K^+, AA^+ (cationic amino acid) and G^- at 50 mmol l^{-1} each with activity coefficients of 10^{-2}]. Here, a strong AA^+ accumulation occurs, with some initial acidification followed by a return to pH neutrality. The $\Delta\Psi$ here is low compared with the *in vivo* condition of the midgut apical membrane (Dow and Peacock, 1989). This discrepancy can be accounted for by the presence of gegenions in the simulation which are needed to prevent chaotic behavior when the time increment is conveniently large. In contrast, the apical membranes of the lepidopteran larval midgut are not very permeable to gegenions and V_m is much higher.

H^+ V-ATPase, K^+/H^+ antiporter and gegenion, with a switch

Fig. 6 shows a simulation which mimics the results of an actual experiment performed by Wieczorek *et al.* (1989). $\Delta\Psi$, E_H, E_K and E_G are plotted for a vesicular system containing an H^+ V-ATPase ($g_P=10^{-5}$ S cm^{-2}, $n=2H^+$ per ATP) and a gegenion (G^-) leakage ($g_G=10^{-4}$ S cm^{-2}). The initial solutions both inside and outside the vesicle are the same [activity of $H^+=10^{-7}$ mol l^{-1} with an activity coefficient of 10^{-7} (see note above) and the activities of K^+ and G^- at 5 mmol l^{-1} each with an activity coefficient of 10^{-2} each]. In the first part of the experiment, the antiporter is turned off ($g_A=10^{-30}$ S cm^{-2}). No K^+ movement is observed, but the vesicle acidifies owing to the action of the V-ATPase. $\Delta\Psi$ and E_G develop just as they did in the section above describing the circuit for an H^+ V-ATPase with gegenion (acidification). Again, as in the preceding paragraph, without the gegenion ion leakage, $\Delta\Psi$ would be much higher and the degree of acidification would be considerably less. Fifty seconds into the experiment, the antiporter is turned on ($g_A=10^{-5}$ S cm^{-2}, $m_A=-2K^+$ per H^+) and immediately the acidification is lost and K^+ accumulates owing to the action of the antiporter. This shift

from H^+ to K^+ accumulation and loss of acidification occurs with only a transient perturbation in the development of $\Delta\Psi$ and E_G.

Conclusion

Thinking in terms of integrated pump, porter and channel circuits makes better sense than thinking in terms of sequential primary and secondary active transport mechanisms and passive transport mechanisms. The dynamic approach is required to appreciate fully the interplay of primary and secondary events in a membrane.

This research has been supported in part by Faculty Incentive Grants and Faculty Development Grants from Immaculata College to F.G.M. and by NIH Research Grant AI-30464 to W.R.H. We thank our colleagues at Temple University, Dr Michael G. Wolfersberger and Dr Ranganath Parthasarathy, for critically evaluating the work in progress. We thank them and Dr Clifford Slayman of Yale University, Dr Bruce Stevens of the University of Florida and Mr James Mooney of Immaculata College, who also provided suggestions as we prepared this manuscript. We also thank Mr Daniel J. Harvey for his assistance in preparing the figures.

References

ANDERSON, E. AND HARVEY, W. R. (1966). Active transport by the Cecropia midgut. II. Fine structure of the midgut epithelium. *J. Cell Biol.* **31**, 107–134.

BLITZER, R. (1964). *Basic Pulse Circuits.* New York: McGraw-Hill. 436pp.

BROWN, D., SABOLIC, I. AND GLUCK, S. (1992). Polarized targeting of V-ATPase in kidney epithelial cells. *J. exp. Biol.* **172**, 231–243.

CHATTERJEE, D., CHAKRABORTY, M., LEIT, M., NEFF, L., JAMSAKELLOKUMPU, S., BARTKIEWICS, M., HERNADO, N. AND BARON, R. (1992). The osteoclast proton pump differs in its pharmacology and catalytic subunits from other vacuolar H^+-ATPases. *J. exp. Biol.* **172**, 193–204.

DOW, J. A. T., GOODWIN, S. F. AND KAISER, K. (1992). Analysis of the gene encoding a 16-kDa proteolipid subunit of vacuolar H^+-ATPase from *Manduca sexta* midgut and tubules. *Gene* **122**, 355–360.

DOW, J. A. T., GUPTA, B. L., HALL, T. A. AND HARVEY, W. R. (1994). X-ray microanalysis of elements in frozen-hydrated sections of an electrogenic K^+ transport system: the posterior midgut of tobacco hornworm (*Manduca sexta*) *in vivo* and *in vitro*. *J. Membr. Biol.* **77**, 223–241.

DOW, J. A. T. AND PEACOCK, J. M. (1989). Microelectrode evidence for the electrical isolation of goblet cell cavities in *Manduca sexta* middle midgut. *J. exp. Biol.* **143**, 101–114.

EDMINISTER, J. A. (1965). *Theory and Problems of Electric Circuits.* New York: Schaum Publishing. 289pp.

EHRENFELD, J., LACOSTE, I. AND HARVEY, B. J. (1989). The key role of the mitochondria-rich cell in Na^+ and H^+ transport across frog skin epithelium. *Pflügers Arch.* **414**, 59–67.

GERENCSER, G. A. AND STEVENS, B. R. (1994). Thermodynamics of symport and antiport catalyzed by cloned or native transporters. *J. exp. Biol.* **196**, 59–75.

GILL, S. S. AND ROSS, L. S. (1990). Molecular cloning and characterization of the B subunit of a vacuolar H^+ATPase from the midgut and Malphigian tubules of *Helicoverpa virescens*. *Archs Biochem. Biophys.* **291**, 92–99.

GOLDMAN, D. E. (1943). Potential, impedance and rectification in membranes. *J. gen. Physiol.* **27**, 37–60.

GRÄF, R., HARVEY, W. R. AND WIECZOREK, H. (1994*a*). Cloning, sequencing and expression of cDNA encoding an insect V-ATPase subunit E. *Biochim. biophys. Acta* **1190**, 193–196.

GRÄF, R., LEPIER, A., HARVEY, W. R. AND WIECZOREK, H. (1994*b*). A novel 14-kDa V-ATPase subunit in the tobacco hornworm midgut. *J. biol. Chem.* **269**, 3767–3774.

GRÄF, R., NOVAK, F. J. S., HARVEY, W. R. AND WIECZOREK, H. (1992). Subunit A of insect plasma membrane V-ATPase has high sequence homology with corresponding subunits from eukaryotic vacuolar membranes. *FEBS Lett.* **300**, 119–122.

GRINSTEIN, S., NANDA, A., LUKACS, G. AND ROTSTEIN, O. (1992). V-ATPases in phagocytic cells. *J. exp. Biol.* **172**, 179–192.

HARVEY, W. R. (1992). Physiology of V-ATPases. *J. exp. Biol.* **172**, 1–17.

HARVEY, W. R., CIOFFI, M. AND WOLFERSBERGER, M. G. (1986). Transport physiology of lepidopteran midgut in relation to the action of By delta-endotoxin. In *Fundamental and Applied Aspects of Invertebrate Pathology* (ed. R. A. Samson, J. M. Vlak and D. Peters), pp. 11–14. Fndn IVth Internat. Colloq. Invert. Pathol., Wageningen, The Netherlands.

HARVEY, W. R. AND NEDERGAARD, S. (1964). Sodium-independent active transport of potassium in the isolated midgut of the *Cecropia* silkworm. *Proc. natn. Acad. Sci. U.S.A.* **51**, 757–765.

HARVEY, W. R. AND NELSON, N. (eds). (1992). *V-ATPases*. *J. exp. Biol.* **172**. 485pp.

HENNIGAN, B. B., WOLFERSBERGER, M. G. AND HARVEY, W. R. (1993*a*). Neutral amino acid symport in larval *Manduca sexta* brush border membrane vesicles deduced from cation dependent uptake of leucine, alanine and phenylalanine. *Biochim. biophys. Acta* **1148**, 216–222.

HENNIGAN, B. B., WOLFERSBERGER, M. G., PARTHASARATHY, R. AND HARVEY, W. R. (1993*b*). Cation dependent leucine, alanine and phenylalanine uptake at pH 10 in brush border membrane vesicles from larval *Manduca sexta* midgut. *Biochim. biophys. Acta* **1148**, 209–215.

HODGKIN, A. L. AND HUXLEY, A. F. (1952). A quantitative description of membrane current and its application to conduction and excitation in nerve. *J. Physiol., Lond.* **117**, 500–544.

HODGKIN, A. L. AND KATZ, B. (1949). The effect of sodium ions on the electrical activity of the giant axon of the squid. *J. Physiol., Lond.* **108**, 37–77.

KEDEM, O. AND KATCHALSKY, A. (1958). Thermodynamic analysis of the permeability of biological membranes to non-electrolytes. *Biochim. biophys. Acta* **27**, 229–246.

KISHIMOTO, U., KAMI-IKE, N. AND TAKEUCHI, Y. (1981). A quantitative expression of the electrogenic pump and its possible role in the excitation of *Chara* internodes. In *The Biophysical Approach to Excitable Systems* (ed. W. J. Adleman and D. E. Goldman), pp. 165–181. New York: Plenum Press.

KLEIN, U. (1992). The insect V-ATPase, a plasma membrane proton pump energizing secondary active transport: immunological evidence for the occurrence of a V-ATPase in insect ion-transporting epithelia. *J. exp. Biol.* **172**, 345–354.

LEPIER, A., AZUMA, M., HARVEY, W. R. AND WIECZOREK, K. (1994). K^+/H^+ antiport in the tobacco hornworm midgut: the K^+-transporting component of the K^+ pump. *J. exp. Biol.* **196**, 361–373.

MANDEL, L. J., MOFFETT, D. F., RIDDLE, T. G. AND GRAFTON, M. M. (1980). Coupling between oxidative metabolism and active transport in the midgut of the tobacco hornworm. *Am. J. Physiol.* **238**, C1–C9.

MARTIN, F. G. (1992). Circuit analysis of transmembrane voltage relationships in V-ATPase-coupled ion movements. *J. exp. Biol.* **172**, 387–402.

MULLENS, L. J. AND NODA, K. (1963). The influence of sodium-free solutions on the membrane potential of frog muscle fibers. *J. gen. Physiol.* **47**, 117–132.

NELSON, N. (1994). Energizing porters by proton-motive force. *J. exp. Biol.* **196**, 7–14.

NOVAK, F. S., GRÄF, R., WARING, R. G., WOLFERSBERGER, M. G., WIECZOREK, H. AND HARVEY, W. R. (1992). Primary structure of V-ATPase subunit B from *Manduca sexta* midgut. *Biochim. biophys. Acta* **1132**, 67–71.

SNELL, F. M., SHULMAN, S., SPENCER, R. P. AND MOOS, C. (1965). *Biophysical Principles of Structure and Function.* Redding, MA: Addison-Wesley Publishing. 390pp.

WIECZOREK, H. (1992). The insect V-ATPase, a plasma membrane proton pump energizing secondary active transport: molecular analysis of electrogenic potassium transport in the tobacco hornworm midgut. *J. exp. Biol.* **172**, 335–343.

WIECZOREK, H., PUTZENLECHNER, M., ZEISKE, W. AND KLEIN, U. (1991). A vacuolar type proton pump energizes K^+/H^+ antiport in an animal plasma membrane. *J. biol. Chem.* **266**, 15340–15347.

WIECZOREK, H., WEERTH, S., SCHINDLBECK, M. AND KLEIN, U. (1989). A vacuolar-type proton pump in a vesicle fraction enriched with a potassium transporting plasma membranes from tobacco hornworm midgut. *J. biol. Chem.* **264**, 11143–11148.